Targeting the N-terminus of α-synuclein Monomer Reduces Fibril-induced Aggregation in the Brain

Éva M. Szegő
Technische Universitat Dresden https://orcid.org/0000-0002-2629-2131
Éva M. Szegő
Technische Universitat Dresden
Fabian Boß
Universitatsklinikum Aachen
Daniel Komnig
Universitatsklinikum Aachen
Charlott Gärtner
Technische Universitat Dresden
Lennart Höfs
Technische Universitat Dresden
Hamed Shaykhalishahi
Heinrich-Heine-Universitat Dusseldorf
Michael Wördehoff
Heinrich-Heine-Universitat Dusseldorf
Theodora Saridaki
Universitatsklinikum Aachen
Jörg B. Schulz
Universitatsklinikum Aachen
Wolfgang Hoyer
Heinrich-Heine-Universitat Dusseldorf
Björn H. Falkenburger (bfalken@ukdd.de)
Technische Universitat Dresden

Research article

Keywords: α-synuclein, pre-formed fibrils, protein aggregation, molecular chaperones

Posted Date: July 20th, 2020

DOI: https://doi.org/10.21203/rs.3.rs-41606/v1

Abstract

Background

Removing α-synuclein aggregates or preventing their formation constitutes a plausible strategy against Parkinson's disease (PD). As we recently demonstrated, the β-wrapin protein AS69 binds an N-terminal region in monomeric α-synuclein (aSyn), interferes with fibril nucleation and reduces aSyn aggregates *in vitro* and in a fruit fly model of A53T aSyn toxicity. Here we tested whether AS69 could also reduce aSyn pathology in mammalian neurons and in mouse brain.

Methods

Primary mouse neurons were exposed to pre-formed fibrils (PFF) of human WT aSyn or PFF was injected into the striatum of A30P-aSyn transgenic mice to induce aSyn pathology. Densities of phospho-aSyn positive somatic inclusions and dystrophic neurites, degeneration of dopaminergic axon terminals in the striatum and the glial response were determined.

Results

PFF were readily taken up by primary mouse neurons, and AS69 did not alter PFF uptake. aSyn pathology, as determined by phospho-aSyn staining, was much more pronounced 72 h after PFF addition than after 24 h, and was reduced by AS69. In the striatum, PFF increased aSyn pathology, induced degeneration of dopaminergic axon terminals and glial activation at 90 days after PFF injection. The extent of terminal loss correlated with the density of dystrophic neurites, but not with the number of somatic inclusions. Co-injection of AS69 with PFF abrogated the induction of somatic inclusions and dystrophic neurites, reduced the loss of dopaminergic axon terminals and the reaction of astroglia, but not the effect on microglia.

Conclusion

AS69, an aSyn monomer-binding protein, reduces aSyn pathology and loss of dopaminergic terminals in primary neurons and in a mouse model. Therefore, our data suggests, that small aSyn-monomer binding proteins, such as AS69, could be promising new therapeutic approaches against Parkinson's disease.

Background

Parkinson disease (PD) and other synucleinopathies, such as dementia with Lewy bodies (DLB) and multisystem atrophy (MSA), are characterized by cytoplasmic aggregates of α-synuclein (aSyn). In PD and DLB, the major hallmarks of aSyn pathology are large inclusions in the neuronal soma termed Lewy bodies (LB) and dystrophic neurites with aSyn aggregates termed Lewy neurites (LN). Familial forms of

PD can be caused by point mutations in the aSyn gene, including the A53T and A30P mutations, and by duplication of the aSyn locus. Polymorphisms in the gene encoding aSyn have been identified as risk factors for sporadic PD [1]. Preventing aSyn aggregation and removing aSyn aggregates are thus plausible neuroprotective strategies against synucleinopathies.

Molecular chaperones mediate the folding of newly produced or misfolded proteins and can prevent protein aggregation in both cellular and animal models of various neurodegenerative diseases [2]. While naturally occurring chaperones, e.g. HSP27 or HSP70, interact with aSyn via weak and transient interaction [3], AS69, an engineered β-wrapin, binds monomeric aSyn with high effectivity and high specificity [4]. AS69 wraps around a sequence region of monomeric aSyn that is critical for aggregation, comprising residues 37–54 [4–6], and stabilizes a β-hairpin conformation [4]. AS69 therefore represents a new paradigm in amyloid inhibition. We showed that the complex of AS69 with monomeric aSyn inhibits the proliferation of aSyn fibrils by interfering with primary and secondary nucleation processes [7]. Coexpression of AS69 in cultured cell lines reduced oligomerization and aggregation of both wild-type (WT) and A53T aSyn without altering the total levels of aSyn, suggesting that AS69 modulates the assembly of aSyn but does not induce its clearance. In a fruit fly model of A53T aSyn toxicity, coexpression of AS69 reduced aggregation of aSyn in neurons and rescued locomotor deficit resulting from neuronal aSyn expression.

In order to validate these findings in mammalian neurons, we now tested the effect of AS69 on aSyn aggregate formation induced by the addition of pre-formed fibrils (PFF) made from recombinant human WT aSyn [8]. Furthermore, we tested AS69 in the more complex biological environment of a mammalian brain using transgenic mice expressing in neurons human aSyn with the A30P mutation [9]; these mice develop pathology spontaneously, but late in life. To accelerate aSyn pathology, we therefore injected aSyn PFF into the striatum. AS69 reduced the extent of aSyn pathology, the loss of dopaminergic axon terminals and the reaction of glial cells.

Methods

Recombinant proteins and fibril formation

Human WT α-synuclein protein and AS69 were produced in bacteria and purified as previously described [10]. In the final purification step, WT aSyn was eluted from a Superdex 75 column (GE Healthcare) equilibrated in PBS buffer. PFF were generated using a standard protocol [8]. In brief, 500 µl of a 5 mg/ml solution of aSyn in PBS were incubated in 1.5 ml microcentrifuge tubes on a Thermomixer (Eppendorf) sealed with parafilm for 7 days at 37 °C under constant agitation (1000 rpm). Fibril formation was confirmed by Thioflavin T fluorescence and atomic force microscopy.

Animals and surgery

C57BL6/J-Thy1-A30P-α-synuclein mice [9] have been used in previous studies [11–13]. They were bred as homozygous, housed and handled in a pathogen-free animal facility at 20–24 °C with a 12 h light/dark

cycle, food and water ad libitum, in accordance with guidelines of the Federation for European Laboratory Animal Science Associations (FELASA). Breeding and surgery were approved by the local authorities (Landesamt für Natur, Umwelt und Verbraucherschutz Nordrhein-Westfalen, licence numbers 84.02.04.2015.A027 and 84-02.04.2014.A321).

Mice were identified by three-digit numbers and assigned to one of three experimental groups using random numbers by a technician not involved in the design of the study. The injected solution was prepared freshly on each experimental day from frozen aliquots of the following three stock solutions: sterile phosphate buffer solution (PBS), PFF in PBS at a concentration corresponding to 5 mg/ml aSyn protein, 404 μM AS69 in PBS. After thawing, PFF were diluted in PBS in order to obtain the same PFF concentration both with and without AS69. The final solutions contained (1) PBS only, (2) 1.4 mg/ml α-synuclein equivalent PFF, (3) 1.4 mg/ml α-synuclein equivalent PFF + 98 μM AS69. (98 μM AS69 is roughly equimolar to 1.4 mg/ml α-synuclein.) After dilution, solutions were sonicated at room temperature with 10% power output and 60 pulses of one second each (300 VT; Biologics, Inc., Manassas, VA).

Stereotaxic injection into the right striatum (AP: 1; ML: 1.5 relative to Bregma; DV: 1.55 from dura) and tissue preparations were performed essentially as described earlier [12]. Briefly, 47–57 week old mice (mixed gender) received 2.5 μl of one of the three solutions (PBS, PFF, PFF + AS69) with a flow rate of 0.2 μl/min. Mice were sacrificed 90 days after the injection. Brains were extracted, fixed at 4 °C in 4% paraformaldehyde in PBS for 24 hours and cryoprotected in 30% sucrose in PBS. Free-floating, 30 μm serial coronal sections were collected with a Cryostat (Leica Microsystems, Germany). Brain slices were stored at − 20 °C (30% glycerol, 30% ethylene glycol in 0.1 M PB) until use.

Primary neuronal culture

Primary neuronal cultures were prepared from P1-3 C57BL6/J mouse pups of mixed sex. Briefly, after dissection and trypsinisation, dissociated neurons were plated onto poly-L-ornithine (Sigma) coated glass coverslip (100 000 cells per well in 24-well dishes), and maintained in Neurobasal A medium containing B27 (2%, Invitrogen), glutamax (0.5 mM, Invitrogen) and antibiotics [14]. One third of the medium was changed on every third day, and from the second change, no antibiotics was added. On DIV 12, neurons were incubated with BSA (1 μg/ml, protein control), 50 nM AS69, PFF corresponding to 50 nM aSyn monomer or the same concentration of PFF + 50 nM AS69. Neurons were analysed on day 13 (24 h after adding PFF) or day 15 (72 h after adding PFF). Experiments were repeated 3–4 times (n = 3–4).

Immunostaining

To visualize the α-synuclein pathology, every 6th section of the striatum was first incubated in 0.3% H_2O_2 for 30 minutes to block endogenous peroxidase activity, then in 3% normal goat serum for 60 min. Sections were then incubated with a primary anti-phospho-synuclein antibody (rabbit, 1:500, ab51253, Abcam, overnight, 4 °C) in 3% normal goat serum, followed by incubation with biotinylated secondary antibody (goat anti-rabbit IgG, 1:200, Vector Laboratories BA-1000), and then with Avidin-Biotin Complex (1:100, Vectastain ABC-Kit Standard PK-6100, Vector Laboratories) for 30 minutes at 21 °C each.

Antibody labelling was visualized by exposure to 4 mg/ml 3,3' diaminobenzidine (DAB) (Sigma Aldrich), and 1% (v/v) H_2O_2 in Tris buffer. Sections were mounted on glass slides, counterstained with Hemalaun, dehydrated to Xylene and coverslipped with Entellan (Merck).

To determine density of dopaminergic axon terminals in the striatum, three sections spanning Bregma levels + 0.26 to + 0.98 mm [15] per animal were stained for TH [16]. After blocking (3% normal goat serum, 60 min), sections were incubated in the presence of the primary TH antibody (rabbit; 1:1000, AB152, Merck Millipore, overnight, 4 °C) followed by secondary antibody (Alexa 488 conjugated goat anti-rabbit; 1:1000, Invitrogen, Carlsbad, CA, USA, 60 min). Sections were mounted with Fluoromount-G (Southern Biotech, Birmingham, AL, USA).

To determine neuroinflammation, every sixth striatal sections were incubated in the presence of the astroglia marker GFAP (chicken, 1:2000, ab4674, Abcam) and for the microglia marker Iba1 (rabbit, 1:1000, 019-19741, Wako, overnight, 4 °C). After incubation with fluorescently labelled secondary antibodies (Alexa 488 conjugated goat anti-chicken and Alexa 555 conjugated donkey anti-rabbit, 1:1000, 120 min), sections were counterstained with Hoechst (Thermo Fischer) and mounted with Fluoromount-G. To determine the density of dopaminergic (TH positive) neurons in the substantia nigra, every third section was stained for TH as described for anti-phospho-synuclein (i.e. with DAB), but using the primary TH antibody (1:1000, overnight, 4 °C).

To determine aSyn uptake and pathology in primary neuronal cultures, fixed cells were permeabilized (0.2% Triton X-100), unspecific sites were blocked (2% BSA), and incubated in the presence of the following primary antibodies (4 °C, overnight): anti phospho-aSyn (mouse, 1:1000, 015-25191, Wako), anti human-aSyn (rat, 15G7, 1:500, ALX-804-258-L001, Enzo Life Sciences), anti-affibody (goat, 1:500, Ab50345, Abcam), anti-MAP2 (rabbit, 1:1000, AB5622, Merck). After incubation with fluorescently labelled secondary antibodies (Alexa 405 conjugated donkey anti-rabbit, anti-Alexa 488 conjugated donkey anti-rat, Alexa 555 conjugated donkey anti-goat and Alexa 647 conjugated donkey anti-mouse), coverslips were mounted on glass objective slides (Fluoromount G).

Analysis of aSyn pathology, striatal fiber density and gliosis

To quantify the extent of aSyn pathology in the striatum, we used the StereoInvestigator software (MicroBrightfield Bioscience, Williston, VT) and the optical fractionator method. Every 6th slice of the striatum was stained. In each slice, a grid of 200 µm × 200 µm was placed randomly over the striatum outlined using the 2.5x objective. At each intersection of the grid, a 100 µm × 100 µm counting frame was inspected manually for phospho-aSyn positive somatic inclusions and dystrophic neurites using a 63x oil objective and an Axio Imager 2 microscope (Carl Zeiss Vision, Göttingen, Germany). The investigator carrying out this analysis was not involved in the surgery and unaware of the injection obtained by each animal (identified by three-digit numbers). Counts reflect the number of items estimated by the stereology procedure for each animal.

For quantification of the density of striatal TH-positive fibers, fluorescence 8-bit images were acquired as z-stack (five slices, 1 µm step) using a 60x oil objective (NA 1.35) and an IX81S1F microscope (Olympus, Hamburg, Germany). A maximum intensity projection over z was performed and TH-positive fibres delineated using the auto-threshold function of ImageJ (1.47v; NIH, Bethesda, MD, USA). Fiber density was expressed as percent area. Three section per animal, and five images per section were analysed resulted in a hierarchically nested design. A generalized linear mixed model was applied [13].

For quantification of gliosis, fluorescent images were acquired using a 20x objective (NA 0.8) with an Axio Imager 2 microscope (Zeiss). After adjusting the threshold on the single images (separate for GFAP and for Iba1; ImageJ), area fraction was determined from 2 sections per animal and from 10 images per section (see above).

The number of dopaminergic neurons in the substantia nigra was quantified as previously [16]: TH-positive neurons in the SNc of the right hemisphere were stereologically counted using the optical fractionator method (StereoInvestigator) in every third section (counting frame: 100 × 100 µm, grid size; 200 × 200 µm; oil immersion 63x objective, NA 1.25).

To measure aSyn uptake and pathology, images of primary cultures were acquired with Zeiss Axio Imager 2 using a 100x oil immersion objective (NA 1.4), with a monochrome camera (Axiocam 705 mono, Zeiss). For each experiment and experimental group, a minimum of 10 neurons were selected randomly. Exposure time was kept constant for each staining across all experimental groups. To outline neurons, a mask was created based on the MAP2 channel. In this mask, the area fraction of (a) phospho-aSyn and (b) human aSyn staining was determined, using ImageJ 1.52 h. Images are pseudo coloured for better visualization.

Statistical analysis and data visualisation

For cell cultures, “n” was set to the number of individual experiments, and for the animal experiments, “n” was set to the number of mice. For each experimental condition and experiment, or for each animal, values were summarized by determining the mean. Data are presented as markers for each condition within a single experiment, and for each animal and as mean ± standard deviation. Comparisons were performed one-way or two-way ANOVA using GraphPad Prism 5 (Version 5.01). $p < 0.05$ was considered significant. p values are depicted as * $p < 0.05$; ** $p < 0.01$.

Results

AS69 decreases intracellular aSyn pathology in primary neurons

AS69 is a small (15 kDa) protein that interferes with aSyn aggregation in a substoichiometric way [4, 7]. The mechanism includes the inhibition of secondary nucleation, which is a critical part of the prion-like behaviour of aSyn and defined as the acceleration of aggregation by the propagation of template

aggregates [PMID: 29978862]. To validate our previous findings from cell lines and fruit flies, we used a primary neuronal model of secondary nucleation, where pre-formed fibrils (PFF) of human WT aSyn are added to the neuronal culture medium [8]. In this model, PFFs are readily taken up by neurons, and induce aggregation of endogenous (mouse) aSyn [17–19]. Since AS69 does not dissociate aSyn fibrils [4, 7, 10], we added AS69 as recombinant protein to the culture medium. BSA was used as negative control.

First, we detected intracellular human aSyn 24 hr after PFF treatment (Fig. 1A, B). In accordance with previous work cited above, this finding confirms that PFF are readily taken up by primary mouse neurons. In addition, we determined the extent of aSyn pathology by staining for phospho-aSyn (Fig. 1A, C). Whereas staining for human aSyn increased most strongly within the first 24 h, staining for phospho-synuclein increased mainly between 24 and 72 h. This is consistent with the hypothesis that seeding of aSyn pathology by PFF takes time. AS69 did not alter the amount of human aSyn at 24 h (Fig. 1B), indicating that AS69 does not affect aSyn uptake. This is in agreement with our previous finding that AS69 does not directly affect aSyn fibrils [4, 7]. AS69 did reduce the extent of phospho-aSyn pathology at 72 h (Fig. 1C), consistent with our previous finding that AS69 reduces secondary nucleation. AS69 also reduced the staining for human aSyn at 72 h (see discussion).

AS69 was added extracellularly and changed intracellular aSyn pathology. To address whether AS69 can be taken up by neurons, we stained for AS69 in cells exposed to AS69 but not PFF. Indeed, AS69 was found inside the neurons (Fig. 1A, BSA + AS69 group), indicating that it can be taken up independently from PFF. Of note, AS69 alone did not induce aSyn pathology (Fig. 1C).

The intracellular area positive for human aSyn staining increased strongly between 24 and 72 h (Fig. 1B). This is not explained by the findings discussed so far. We cannot rule out that a subtle effect of AS69 on PFF uptake amplifies over time. However, human aSyn PFF induces the aggregation of endogenous mouse aSyn, and the deposition of phospho-aSyn-positive inclusions is rather mouse aSyn-driven [20]. Therefore the difference in human aSyn staining at 72 h is better explained by the fact that the particles revealed by human aSyn staining are not only composed of human aSyn but contain endogenous mouse aSyn as well. In other words, the area of human aSyn staining does not faithfully report the amount of intracellular human aSyn protein but rather the area of aSyn pathology containing human aSyn. If the increase in human aSyn staining between 24 and 72 h results from expansion of pathology containing human aSyn, the smaller area with AS69 is explained by reduced seeding of aSyn pathology with AS69. In addition, fewer and smaller aSyn aggregates are easier to degrade, so reduced seeding of aSyn pathology by AS69 could also facilitate clearance of aSyn aggregates.

AS69 reduces PFF-induced α-synuclein pathology in vivo

Taken together, AS69 reduced the amount of aSyn pathology in primary neurons but did not interfere with PFF uptake. To expand on this finding, we asked whether AS69 could also reduce PFF-induced aSyn pathology in mice. To induce a robust aSyn pathology, we injected the same human WT aSyn PFF into the striatum of 47–57 week old mice with neuronal expression of human A30P-αSyn [9]. aSyn transgenic mice were used because in these mice neurons express more aSyn, which facilitates initiation of aSyn

pathology. Brains were analysed 90 days after the injection (Fig. 2A). To reveal striatal aSyn pathology induced by PFF injection, we visualized phospho-aSyn positive structures (Fig. 2B) and discriminated two phenotypes: (1) Somatic Accumulations of phospho-aSyn staining (“SA”, solid arrows in Fig. 2B) and (2) Dystrophic, phospho-aSyn positive Neurites (“DN”, open arrows in Fig. 2B). These changes are reminiscent of the somatic Lewy bodies and Lewy neurites in human brain, respectively. Numbers of SA and DN in each striatum were determined by stereology.

Even in vehicle-injected mice we saw a relevant number of striatal SA (Fig. 2B, C) and DN (Fig. 2B, D) and attribute this to the neuronal overexpression of A30P-aSyn in this mouse line. In PFF-injected striatum we observed more SAs (Fig. 2C) and DNs (Fig. 2D) than in the contralateral striatum, indicating that PFF induced additional aSyn pathology. Of note, the extent to which PFF injection increased phospho-aSyn pathology differed between SA and DN: The ratio between the injected and non-injected hemispheres was significantly different from the control for DN but not for SA (Fig. 2C, D). In accordance with our *in vitro* findings (Fig. 1C), co-injection of AS69 with the PFF prevented the induction of aSyn pathology: With AS69, the number of SA and DN was not different between the ipsi- and contralateral hemispheres (Fig. 2C, D), and the ratio between both hemisphere did not differ from control (Supplementary Fig. 1A, B).

PFF-induced degeneration of dopaminergic axon terminals

A30P-α-synuclein transgenic mice do not show spontaneous degeneration of dopaminergic neurons in the substantia nigra or degeneration of their axon terminals in the striatum [11]. Yet, the injection of PFF into the striatum reduced the density of dopaminergic axon terminals by about 20% (Fig. 3A, B; absolute densities of each hemispheres are shown in Supplementary Fig. 1C). Co-injection of AS69 prevented the PFF-induced degeneration of dopaminergic axon terminals (Fig. 3A, B). The number of dopaminergic cell bodies in the *substantia nigra pars compacta* was not significantly altered by PFF injection into the striatum or co-injection of AS69 (data not shown).

Although it is widely accepted that aSyn pathology is a major hallmark of PD and driver of neurodegeneration, it is still a matter of debate which type of aSyn pathology better correlates with neurotoxicity and functional impairment [21]. Therefore, we correlated on an animal basis the extent of SA and DN with the density of dopaminergic axon terminals. Interestingly, while the increase of round, somatic, Lewy-body-like SA showed no correlation with dopaminergic fiber loss (Fig. 3C), we observed a strong correlation between the number of DNs and the reduction in dopaminergic axon terminals (Fig. 3D). This difference suggests that neuritic aSyn pathology is more closely linked to the degeneration of dopaminergic axon terminals than somatic accumulations.

Response of glial cells to PFF injection

To determine to what extent glial cells respond to PFF injection, we stained striatal sections for the microglial marker Iba1 or the astroglial marker GFAP (Fig. 4A). PFF injection induced a significant activation of both microglia (Fig. 4B) and astroglia (Fig. 4C). Injection of PBS alone did not produce a significant glial activation, confirming that that the observed effects can indeed be attributed to the PFF and are not a nonspecific response to the intracerebral injection. AS69 did not moderate the Iba1

response (Fig. 4B). Accordingly, the Iba1 response did not correlate with the reduction in dopaminergic fibers (supplemental Figure S1G), or with the extent of DN and SA pathology (supplemental Figure S1H, I). Activation of astroglia, in contrast, was significantly reduced by AS69 (Fig. 4C). Moreover, the extent of astroglial activation correlated inversely with the density of dopaminergic fibers (Fig. 4D) and correlated positively with the relative density of DNs (Fig. 4E). The extent of astroglial activation did not correlate with the density of SA (supplemental Fig. 1F).

Discussion

aSyn aggregates are the main fibrillary components of Lewy neurites and Lewy bodies, and targeting those aggregates might hold therapeutic potential. In our previous studies [4, 7, 10] we reported on a novel strategy to inhibit aSyn nucleation by using a high affinity monomer binding molecule, AS69. Here, we investigated the effect of AS69 in PFF-based *in vivo* models of synucleinopathies. We show, that AS69 did not alter PFF uptake in primary neurons, but it reduced PFF-induced aSyn pathology. In mice, AS69 ameliorated PFF-induced aSyn pathology in the striatum, loss of dopaminergic axon terminals and astroglia activation.

Chronic overexpression of human A30P aSyn and acute injection of PFF from human WT aSyn trigger morphologically distinct types of aSyn pathology (Fig. 2C, D). We propose that neurons with chronic overexpression of human A30P aSyn can still maintain retrograde transport and collect aSyn aggregates in perinuclear accumulations (SAs). Indeed, in the A30P mice without PFF injection, basal aSyn pathology is mostly restricted to somatic accumulations (SAs, reminiscent of LBs) with only few dystrophic neurites (DNs, reminiscent of LNs), consistent with earlier studies [22]. These mice do not show a loss of dopaminergic somata in the substantia nigra, degeneration of dopaminergic axon terminals in the striatum or glial activation (Figs. 2B, 3A and reference [11]), but their neurons are vulnerable [13, 22–24]. Toxic insults, such as MPTP or PFF disrupt retrograde transport and damage neurite integrity. Accordingly, injection of PFF into A30P mice induced a robust increase in aSyn pathology, consistent with previous work for other aSyn transgenic mice [25, 26]. The PFF-induced increase in the number of DN was much more pronounced than for SA (Fig. 2C,D). This formation of DN may result from excessive seeding of aSyn aggregates in neurites and from impaired transport of aSyn aggregates to the soma. Damaged neurites can explain the loss of dopaminergic axon terminals in the striatum, a causal relationship is supported by the tight correlation of DN with dopaminergic fiber loss (Fig. 3D). In the striatum, dopaminergic axon terminals are particularly vulnerable because they are far from the neuronal soma, and because dopamine further increases aSyn aggregation [27, 28]. Still, we expect that not all DN we observed are dopaminergic, and that PFF also trigger aSyn aggregation in non-dopaminergic neurites. AS69 reduced DN (Fig. 2D) and we propose that this underlies the higher density of remaining axon terminals (Fig. 3B).

Neurodegeneration and the presence of aSyn pathology are often accompanied by activation of glial cells [29, 30]. We found a moderately increased microglia activation in aSyn transgenic animals (Fig. 4A), consistent with previous studies using the same mouse line [30]. PFF injection led to an activation of

both glia types, but the extent of microglia activation did not correlate with the amount of synuclein pathology (DAs or SAs) or with neuronal damage, represented by dopaminergic fiber loss (Supplementary Figure G-I). This suggests that in this animal model, microglia do not have a direct role in neuronal damage, even though aggregated aSyn is a potent activator of microglia in other paradigms [31, 32]. In contrast, astroglia was not activated in controls, but increased with PFF (Fig. 4A). The extent of astroglia activation correlated with the number of DN and with the density of dopaminergic fibers, suggesting an involvement of astroglia in PFF-induced neuronal damage (Fig. 4D, E); further work will be required to determine the role of astroglia activation. Consistent with the involvement of astroglia but not microglia in aSyn dependent damage, AS69 reduced astrogliosis but did not affect microglia activation.

What is the cellular mechanism of AS69? In mouse primary neurons exposed to PFF with either BSA or AS69 for 24 h, we detected the same amount of intracellular human aSyn (Fig. 1B). We therefore assume that AS69 does not influence uptake of PFF, consistent with our previous finding that AS69 does not induce disassembly of higher order aSyn species [4]. We also showed that neurons take up AS69 (Fig. 1A), similar to other proteins [27], allowing the protective effects of AS69 to be explained by intracellular events. With AS69, the amount of phospho-aSyn 72 h after adding PFF to cultured neurons was significantly smaller (Fig. 1C), consistent with the lower number of DN in mice (Fig. 2D) and in drosophila neurons (Agerschou et al., 2019). Based on our previous findings that the complex of AS69 and aSyn inhibits secondary nucleation and aggregate amplification [7] the most probable mechanism of AS69 is to prevent seeding of aSyn pathology by binding intracellular aSyn monomers.

Conclusions

Taken together, we demonstrated that the quantification of DNs, dopaminergic axon terminals and astrogliosis are sensitive measures of neuronal damage in our animal model. AS69 reduced the induction of aSyn pathology by PFF, reduced the loss of dopaminergic fibers and decreases astrogliosis. Prevention of seeding of aSyn pathology by monomer sequestration might therefore represent a plausible therapeutic strategy for synucleinopathies.

Abbreviations

aSyn
alpha-synuclein; BSA:bovine serum albumin; DLB:dementia with Lewy bodies; DN:distrophic neurite; GFAP:glial fibrillary acidic protein; HSP27/70:heat shock protein 27/70; Iba1:ionized calcium-binding adapter molecule 1; LB:Lewy body; LN:Lewy neurite; MSA:multisystem atrophy; PBS:phosphate buffered saline solution; PD:Parkinson`s disease; PFF:pre-formed fibrils; SA:somatic accumulation; TH:tyrosine hydroxylase; WT:wild-type

Declarations

Ethical Approval and Consent to participate

Breeding and surgery were approved by the local authorities (Landesamt für Natur, Umwelt und Verbraucherschutz Nordrhein-Westfalen, licence numbers 84.02.04.2015.A027 and 84-02.04.2014.A321).

Consent for publication

All authors approved the manuscript.

Availability of data and materials

All relevant data are included in the main text and in supplemental Figure S1. The number of TH positive neurons in the substantia nigra is available upon request.

Competing interests

The authors declare that they have no competing interests.

Funding

This work was supported by the German Research Foundation (DFG, FA 658/3 – 1, to BF) and by the Interdisciplinary Center for Clinical Research (IZKF) Aachen (to TS). Support by a European Research Council (ERC) Consolidator Grant (grant agreement no. 726368, to WH) is acknowledged.

Authors' contributions

EMSz, JS, WH and BHF conceived research, EMSz, FB, DK, CG, LH, HS, MW, TS performed research, EMSz, WH and BF wrote the first draft of the manuscript, all authors contributed and approved the manuscript.

Acknowledgements

We thank Sabine Hamm for excellent technical assistance and Akanksha Nagpal, Natalie Gasterich for their contributions to this project.

References

1. Klein C, Westenberger A. Genetics of Parkinson’s disease. Cold Spring Harb Perspect Med. Cold Spring Harbor Laboratory Press; 2012;2.
2. Muchowski PJ, Wacker JL. Modulation of neurodegeneration by molecular chaperones. Nat. Rev. Neurosci. Nature Publishing Group; 2005. p. 11–22.

3. Jia C, Ma X, Liu Z, Gu J, Zhang X, Li D, et al. Different Heat Shock Proteins Bind α-Synuclein With Distinct Mechanisms and Synergistically Prevent Its Amyloid Aggregation. Front Neurosci. Frontiers Media S.A.; 2019;13.
4. Mirecka EA, Shaykhalishahi H, Gauhar A, Akgül Ş, Lecher J, Willbold D, et al Sequestration of a β-hairpin for control of α-synuclein aggregation. Angew Chemie - Int Ed [Internet]. Wiley-VCH Verlag; 2014 [cited 2020 Apr 29];53:4227–30.
5. Doherty CPA, Ulamec SM, Maya-Martinez R, Good SC, Makepeace J, Khan GN, et al. A short motif in the N-terminal region of α-synuclein is critical for both aggregation and function. Nat Struct Mol Biol [Internet] Nature Research. 2020;27:249–59. [cited 2020 Jun 25 ;.
6. Shaykhalishahi H, Gauhar A, Wördehoff MM, Grüning CSR, Klein AN, Bannach O, et al. Contact between the β1 and β2 Segments of α-Synuclein that Inhibits Amyloid Formation. Angew Chemie - Int Ed [Internet]. Wiley-VCH Verlag; 2015 [cited 2020 Jun 25];54:8837–40.
7. Agerschou ED, Flagmeier P, Saridaki T, Galvagnion C, Komnig D, Heid L, et al. An engineered monomer binding-protein for α-synuclein efficiently inhibits the proliferation of amyloid fibrils. Elife [Internet]. eLife Sciences Publications Ltd; 2019 [cited 2019 Oct 25];8.
8. Volpicelli-Daley LA, Luk KC, Lee VM-Y. Addition of exogenous α-synuclein preformed fibrils to primary neuronal cultures to seed recruitment of endogenous α-synuclein to Lewy body and Lewy neurite-like aggregates [Internet]. Nat. Protoc. 2014 [cited 2018 Mar 16]. p. 2135–46.
9. Kahle PJ, Neumann M, Ozmen L, Muller V, Jacobsen H, Schindzielorz a, et al. Subcellular localization of wild-type and Parkinson's disease-associated mutant alpha -synuclein in human and transgenic mouse brain. J Neurosci. 2000;20:6365–73.
10. Gauhar A, Shaykhalishahi H, Gremer L, Mirecka EA, Hoyer W. Impact of subunit linkages in an engineered homodimeric binding protein to α-synuclein. Protein Eng Des Sel Oxford Academic. 2014;27:473–9.
11. Rathke-Hartlieb S, Kahle PJ, Neumann M, Ozmen L, Haid S, Okochi M, et al. Sensitivity to MPTP is not increased in Parkinson' s disease-associated mutant α-synuclein transgenic mice. J Neurochem. 2001;77:1181–4.
12. Krenz A, Falkenburger BH, Gerhardt E, Drinkut A, Schulz JB. Aggregate formation and toxicity by wild-type and R621C synphilin-1 in the nigrostriatal system of mice using adenoviral vectors. J Neurochem [Internet]. John Wiley & Sons, Ltd (10.1111); 2009 [cited 2019 Oct 29];108:139–46.
13. Szegő ÉM, Gerhardt E, Kermer P, Schulz JB. A30P α-synuclein impairs dopaminergic fiber regeneration and interacts with L-DOPA replacement in MPTP-treated mice. Neurobiol Dis [Internet]. 2012;45:591–600. [cited 2016 Jan 6 ;.
14. Szegő ÉM, Dominguez-Meijide A, Gerhardt E, König A, Koss DJ, Li W, et al. Cytosolic Trapping of a Mitochondrial Heat Shock Protein Is an Early Pathological Event in Synucleinopathies. Cell Rep [Internet]. 2019;28:65–77.e6. [cited 2019 Oct 29 ;.
15. Paxinos G, Franklin KBJ. Paxinos and Franklin's the Mouse Brain in Stereotaxic Coordinates. Acad. Press. 2001.

16. Komnig D, Schulz JB, Reich A, Falkenburger BH. Mice lacking Faim2 show increased cell death in the MPTP mouse model of Parkinson disease. J Neurochem Blackwell Publishing Ltd. 2016;139:848–57.
17. Wu Q, Takano H, Riddle DM, Trojanowski JQ, Coulter DA, Lee VMY. α-Synuclein (αsyn) preformed fibrils induce endogenous αsyn aggregation, compromise synaptic activity and enhance synapse loss in cultured excitatory hippocampal neurons. J Neurosci Society for Neuroscience. 2019;39:5080–94.
18. Karpowicz RJ, Haney CM, Mihaila TS, Sandler RM, Petersson EJ, Lee VMY. Selective imaging of internalized proteopathic -synuclein seeds in primary neurons reveals mechanistic insight into transmission of synucleinopathies. J Biol Chem. American Society for Biochemistry and Molecular Biology Inc.; 2017;292:13482–97.
19. Villar-Piqué A, Da Fonseca TL, Sant'Anna R, Szegö ÉM, Fonseca-Ornelas L, Pinho R, et al. Environmental and genetic factors support the dissociation between α-synuclein aggregation and toxicity. Proc Natl Acad Sci U S A. National Academy of Sciences; 2016;113:E6506–15.
20. Okuzumi A, Kurosawa M, Hatano T, Takanashi M, Nojiri S, Fukuhara T, et al. Rapid dissemination of alpha-synuclein seeds through neural circuits in an in-vivo prion-like seeding experiment. Acta Neuropathol Commun [Internet] NLM (Medline); 2018 [cited 2020 Jun 17];6:96.
21. Schulz-Schaeffer WJ. Neurodegeneration in Parkinson disease: Moving Lewy bodies out of focus. Neurology. Lippincott Williams and Wilkins; 2012. p. 2298–9.
22. Ekmark-Lewén S, Lindström V, Gumucio A, Ihse E, Behere A, Kahle PJ, et al. Early fine motor impairment and behavioral dysfunction in (Thy-1)-h[A30P] alpha-synuclein mice. Brain Behav. John Wiley and Sons Ltd; 2018;8.
23. Szegő ÉM, Outeiro TF, Kermer P, Schulz JB. Impairment of the septal cholinergic neurons in MPTP-treated A30P α-synuclein mice. Neurobiol Aging [Internet]. Elsevier; 2013 [cited 2016 Jan 6];34:589–601.
24. Unal-Cevik I, Gursoy-Ozdemir Y, Yemisci M, Lule S, Gurer G, Can A, et al. Alpha-synuclein aggregation induced by brief ischemia negatively impacts neuronal survival in vivo: A study in A30Palpha-synuclein transgenic mouse. J Cereb Blood Flow Metab Nature Publishing Group. 2011;31:913–23.
25. Zhang B, Kehm V, Gathagan R, Leight SN, Trojanowski JQ, Lee VMY, et al. Stereotaxic targeting of alpha-synuclein pathology in mouse brain using preformed fibrils. Methods Mol Biol. Humana Press Inc.; 2019. p. 45–57.
26. Luk KC, Kehm V, Carroll J, Zhang B, Brien PO, Trojanowski JQ, et al. Pathological a-synuclein transmission initiates Parkinson-like neurodegeneration in nontransgenic mice. Science. 2012;338:949–54.
27. Mor DE, Tsika E, Mazzulli JR, Gould NS, Kim H, Daniels MJ, et al. Dopamine induces soluble α-synuclein oligomers and nigrostriatal degeneration. Nat Neurosci Nature Publishing Group. 2017;20:1560–8.

28. Conway KA, Rochet JC, Bieganski RM, Lansbury J. Kinetic stabilization of the α-synuclein protofibril by a dopamine-α-synuclein adduct. Science (80-) Science. 2001;294:1346–9.
29. Refolo V, Stefanova N. Neuroinflammation and glial phenotypic changes in alpha-synucleinopathies. Front. Cell. Neurosci. Frontiers Media S.A.; 2019.
30. Filippini A, Gennarelli M, Russo I. α-Synuclein and Glia in Parkinson's Disease: A Beneficial or a Detrimental Duet for the Endo-Lysosomal System? Cell. Mol. Neurobiol. Springer New York LLC; 2019. p. 161–8.
31. Klegeris A, Pelech S, Giasson BI, Maguire J, Zhang H, McGeer EG, et al. α-Synuclein activates stress signaling protein kinases in THP-1 cells and microglia. Neurobiol Aging Elsevier. 2008;29:739–52.
32. Gustot A, Gallea JI, Sarroukh R, Celej MS, Ruysschaert JM, Raussens V. Amyloid fibrils are the molecular trigger of inflammation in Parkinson's disease. Biochem J Portland Press Ltd. 2015;471:323–33.

Figures

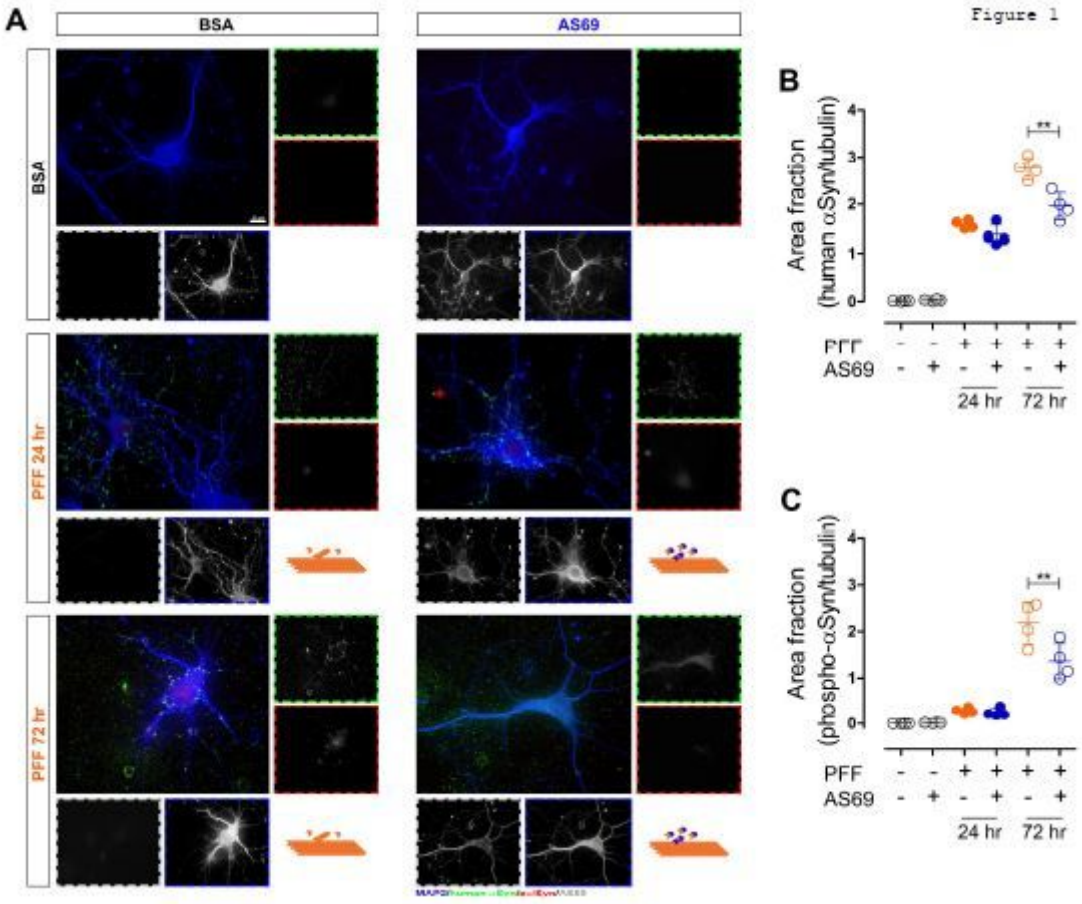

Figure 1

AS69 inhibits PFF-induced aggregation of endogenous aSyn monomers in primary neurons. (A) Representative images of primary neurons treated with (BSA or AS69) and (BSA or PFF) 24 hrs and 72

hrs after treatment. Immunostaining for AS69 (white), phospho-aSyn (red) and human aSyn(green) were detected within neurons visualized with an antibody cocktail of neuronal markers (MAP2 and βIII-tubulin, blue). Scale bar: 10 µm. (B) Quantification of human aSyn within neurons 24 hrs and 72 hrs after seeding with PFF. (C) Quantification of phospho-aSyn within primary neurons. Markers on graphs represent mean area fractions obtained for individual experiments (n=4). Lines represent mean ± SD. **: p<0.01, two-way ANOVA.

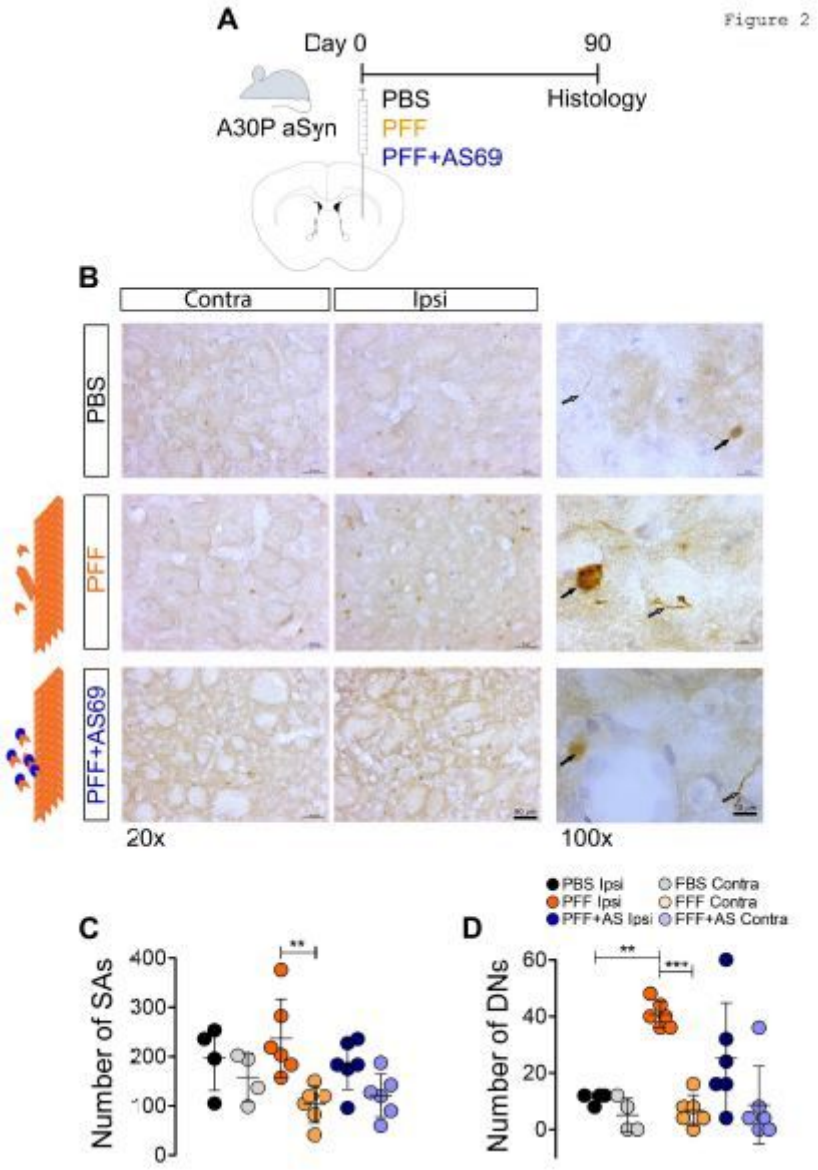

Figure 2

AS69 inhibits PFF-induced aSyn-pathology in the mouse brain. (A) Injection scheme: transgenic mice expressing human aSyn with the A30P mutation [9] were injected with PBS as control; PFF prepared from WT aSyn or with PFF+AS69 protein together. aSyn-induced pathology was analysed 90 days after injection. (B) Representative, low (20x) and high (100x) magnification images showing paSyn-positive structures in the striatum. Distrophic neurites (DN, open arrows) and somatic accumulations (SA, black arrows) were counted separately in the striatum. Scale bars: 50 µm (20x) and 10 µm (100x).

Quantification of SAs (C) and DNs (D) show, that only PFF injection induced accumulation of paSyn-positive structures in the striatum. Dark colours: ipsilateral, light colours: contralateral striatum. Markers on graphs represent individual animals. Lines represent mean ± SD. **: p<0.01; ***: p<0.001, two-way ANOVA.

Figure 3

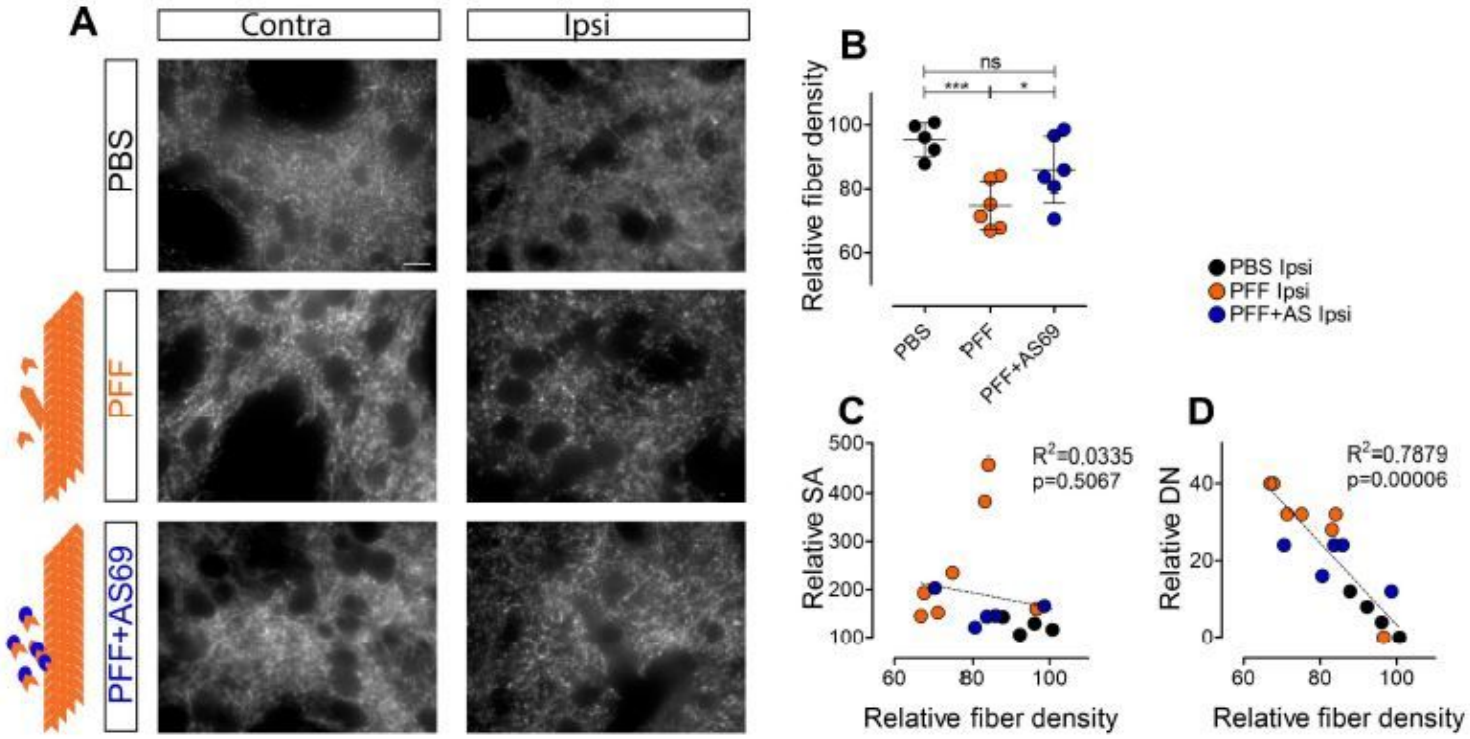

Figure 3

AS69 decreases PFF-induced reduction of striatal dopaminergic fibers. (A) Representative images showing dopaminergic (TH positive)fibers in the striatum 90 days after PFF injection. Scale bar: 10 µm. (B)Relative density of striatal dopaminergic fibers in the striatum(ratio ipsilateral/contralateral) shows that co-injection of AS69 decreases PFF-induced fiber loss. Data for individual hemispheres are in Supplementary Figure 1C.(C) Linear regression between relative density of dopaminergic fibers and relative SA (ipsilateral/contralateral), showing no significant correlation. (D) Linear regression between relative density of dopaminergic fibers and relative DN (ipsilateral-contralateral).Markers on graphs represent individual animals. Lines represent mean ± SD. **: p<0.01; ***: p<0.001, one-way ANOVA (B), linear regression (C, D).

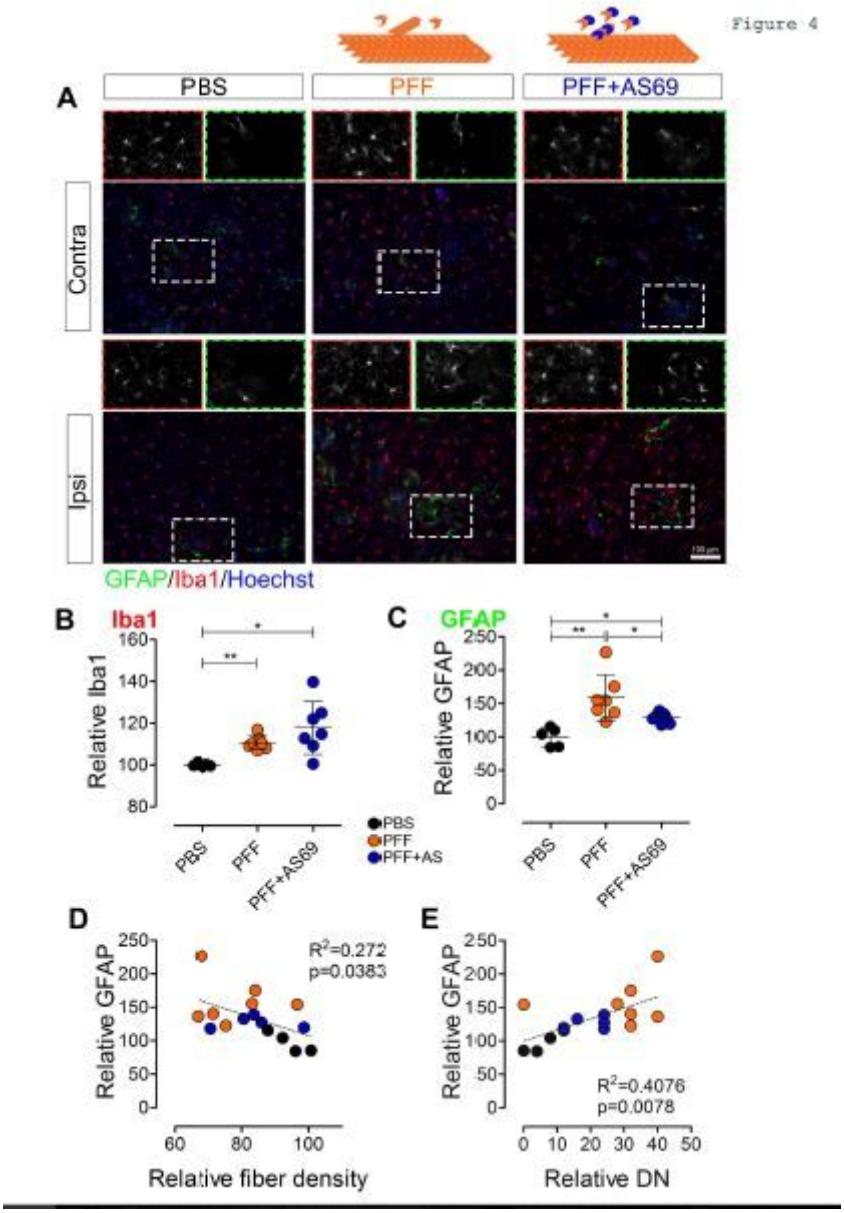

Figure 4

AS69 decreases PFF-induced astrogliosis in the mouse brain. (A) Representative images showing astroglia (labelled with GFAP, green) and microglia (Iba1, red) in the striatum of transgenic mice 90 days after PFF injection. Scale bar: 100 µm. (B) Relative microglia reaction (ipsilateral/contralateral). AS69 had no effect on PFF-induced microgliosis. Data for individual hemispheres are in Supplementary Figure 1D. (C) Relativeastroglia reaction (ipsilateral/contralateral). Co-injection of AS69 decreased PFF-induced astrogliosis. Data for individual hemispheres are in Supplementary Figure 1D. (D) Linear regression shows negative correlation between astroglia reaction and relative density of dopaminergic fibers. (E) Linear regression shows positive correlation between astroglia reaction and relative DN number. Markers on graphs represent individual animals. Lines represent mean ± SD. *: p<0.05; **: p<0.01, one-way ANOVA (B, C), linear regression (D, E).

Supplementary Files

This is a list of supplementary files associated with this preprint. Click to download.

- FigS1.JPG